# Characterization of 2‘-Deoxycytidine Adducts Derived from 4-Oxo-2-nonenal, a Novel Lipid Peroxidation Product

**ARTICLE** *in* CHEMICAL RESEARCH IN TOXICOLOGY · AUGUST 2003

Impact Factor: 3.53 · DOI: 10.1021/tx030009p · Source: PubMed



**6 AUTHORS**, INCLUDING:

Tomoyuki Oe
Tohoku University
**80** PUBLICATIONS **1,652** CITATIONS
SEE PROFILE

Seon Hwa Lee
Tohoku University
**76** PUBLICATIONS **2,465** CITATIONS
SEE PROFILE

Maria Victoria Silva Elipe
Amgen
**34** PUBLICATIONS **1,256** CITATIONS
SEE PROFILE

Ian A Blair
University of Pennsylvania
**428** PUBLICATIONS **12,435** CITATIONS
SEE PROFILE

# Characterization of 2′-Deoxycytidine Adducts Derived from 4-Oxo-2-nonenal, a Novel Lipid Peroxidation Product

Michael Pollack,[†] Tomoyuki Oe,[†] Seon Hwa Lee,[†] Maria Victoria Silva Elipe,[‡] Byron H. Arison,[‡] and Ian A. Blair*,[†]

*Center for Cancer Pharmacology, University of Pennsylvania School of Medicine, 1254 BRB II/III, 421 Curie Boulevard, Philadelphia, Pennsylvania 19104-6160, and Department of Drug Metabolism, Merck Research Laboratories, P.O. Box 2000, RY80L-109, Rahway, New Jersey 07065*

*Received February 28, 2003*

Analysis of the reaction between 2′-deoxycytidine and 4-oxo-2-nonenal by LC/MS revealed the presence of three major products (adducts $A_1$, $A_2$, and B; $[M + H]^+ = 364$). Adducts $A_1$ and $A_2$ were isomeric, and each dehydrated to form adduct B. The structure of adduct B was shown by LC/MS and NMR spectroscopy to be an etheno-2′-deoxycytidine adduct 1″-[1-(2′-deoxy-β-D-*erythro*-pentofuranosyl)-1H-imidazo[2,1-c]pyrimidin-2-oxo-4-yl]heptane-2″-one. A time course experiment performed at 65 °C (pH 5−8) showed that the transformation of both $A_1$ and $A_2$ was pH-dependent. In acidic conditions, adducts $A_1$ and $A_2$ dehydrated primarily to adduct B. In contrast, in basic conditions, adducts $A_1$ and $A_2$ hydrolyzed primarily to dCyd. The data are consistent with adducts $A_1$ and $A_2$ being substituted ethano adducts that dehydrate to adduct B, a substituted 3,$N^4$-etheno-2′-deoxycytidine adduct.

## Introduction

Oxidative stress is thought to play an important role in the development of degenerative diseases of aging such as cancer (*1, 2*). The decline in cellular reducing equivalents during oxidative stress allows the accumulation of PUFA[1] lipid hydroperoxides. The subsequent homolytic decomposition of these hydroperoxides results in the formation of aldehydic bifunctional electrophiles that covalently modify DNA. PUFA lipid hydroperoxides are formed nonenzymatically by reactive oxygen species (*3*). They are also formed as specific products of LOXs and COXs, enzymes that are upregulated in cancer (*4*, *5*).

Transition metal ions such as $Fe^{II}$ and $Cu^{I}$ induce homolytic decomposition of the prototypic ω-6 PUFA lipid hydroperoxide 13-HPODE to α,β-unsaturated aldehyde genotoxins, such as 4-hydroxy-2-nonenal and 4-oxo-2-nonenal (*6*). Recently, vitamin C has also been shown to induce PUFA lipid hydroperoxide decomposition to the same aldehydic genotoxins (*7*). These resulting genotoxins form DNA adducts, which have been implicated in mutagenesis and carcinogenesis (*8*, *9*). For example, 4-hydroxy-2-nonenal can react with dGuo to form a tricyclic substituted propano adduct (*10*). Also, 4-oxo-2-nonenal, a recently characterized lipid peroxidation product (*6*), has been shown to react with dAdo and dGuo to form substituted etheno adducts (*11*−*13*).

Etheno adducts were first detected in rodents and humans exposed to vinyl chloride (*14*). Using immunoaffinity purification and $^{32}$P-postlabeling, it was found that these lesions were present in unexposed individuals, apparently as a result of endogenous lipid peroxidation (*15*). In regard to cancer, increased levels of etheno−dCyd adducts were found in colon polyps from patients with familial adenomatous polyposis (*16*) and in the mouse skin two stage model of carcinogenesis (*17*).

Miscoding properties of etheno−dCyd were studied in vitro with the Klenow fragment of DNA polymerase I from *Escherichia coli* (*18*, *19*) and more recently using both typical and atypical mammalian DNA polymerases (*20*, *21*). The mutagenic properties of etheno−dCyd were studied by transfecting plasmid vectors containing site specific adducts into *E. coli* and mammalian cells (*22*−*24*). While etheno−dCyd had a low mutation rate in nonirradiated *E. coli*, it was highly mutagenic in mammalian cells (*24*). Therefore, etheno−dCyd has been proposed to play an important role in the etiology of cancer. In this study, a novel substituted etheno−dCyd adduct produced from the reaction between 4-oxo-2-nonenal and dCyd was characterized using LC/MS and NMR spectroscopy.

## Materials and Methods

**Materials.** dCyd, acetic acid, trifluoroacetic acid, sodium hydrogenphosphate, sodium dihydrogenphosphate, and diethyl ether were purchased from Sigma Chemical Co. (St. Louis, MO). Ammonium acetate was obtained from J. T. Baker (Phillipsburg, NJ). Microcentrifuge tubes (1.5 mL), HPLC grade water, and HPLC grade methanol were obtained from Fisher Scientific Co. (Fair Lawn, NJ). ACS/USP grade ethanol was obtained from Pharmcoproducts Inc. (Brookfield, CT). Gases were supplied by BOC Gases (Lebanon, NJ).

* To whom correspondence should be addressed. Fax: (215)573-9889. E-mail: ian@spirit.gcrc.upenn.edu.
† University of Pennsylvania School of Medicine.
‡ Merck Research Laboratories.

[1] Abbreviations: COSY, $^1$H,$^1$H 2D correlation spectroscopy; CID, collision-induced dissociation; COX, cyclooxygenase; dAdo, 2′-deoxyadenosine; dCyd, 2′-deoxycytidine; dGuo, 2′-deoxyguanosine; DMSO, dimethylsulfoxide; ESI, electrospray ionization; HMBC, $^1$H,$^{13}$C 2D heteronuclear multiple bond correlation; HMQC, $^1$H,$^{13}$C 2D heteronuclear multiple quantum correlation; HSQC, $^1$H,$^{13}$C 2D heteronuclear single quantum correlation; 13-HPODE, 13-hydroperoxy-[S-(*Z*,*E*)]-9,-11-octadecadienoic acid; LOX, lipoxygenase; NOE, nuclear Overhauser effect; PUFA, polyunsaturated fatty acid; ROESY, rotating frame nuclear Overhauser effect; TPA, tetradecanoyl phorbol acetate.

10.1021/tx030009p CCC: $25.00 
Published on Web 06/14/2003

**NMR.** The NMR spectra were determined at 25 °C on a Varian Inova 600 MHz instrument equipped with a Nalorac 3 mm indirect detection gradient probe. $^{13}C$ experiments were carried out at 150 MHz. The sample (1.7 mg) was dissolved in 150 $\mu$L of DMSO-$d_6$. The data processing was performed on the spectrometer. Chemical shifts are reported in the $\delta$ scale (ppm) by assigning the residual solvent peak for DMSO to 2.49 and 39.5 ppm for $^1H$ and $^{13}C$, respectively. The ROESY experiment was determined with a 300 ms mixing time. The delay between successive pulses was 1 s for COSY and ROESY. Both the HSQC and the HMBC spectra were determined using gradient pulses for coherence selection. The HSQC spectrum was determined with decoupling during acquisition. Delays corresponding to one bond $^{13}C-^1H$ coupling (ca. 140 Hz) for the low pass filter and to 2−3 bond $^{13}C-^1H$ long-range coupling (5, 7, or 10 Hz) were used for the HMBC measurements.

**MS.** The data were acquired on a Finnigan TSQ 7000 triple-stage quadrupole mass spectrometer fitted with an ESI source (Thermo Finnigan, San Jose, CA). The mass spectrometer was operated in the positive ion mode with a potential of 4.5 kV applied to the electrospray needle. The capillary temperature was held at 210 °C. Nitrogen was used as the sheath (80 psi) and auxiliary gas (20 psi) to assist with nebulization. Argon was used as the collision gas in CID experiments. Full scanning analyses were performed in the range of *m/z* 150−500. Product ion scanning analyses were performed in the range of *m/z* 50−400.

**LC.** Chromatography was performed using a Waters Alliance 2690 HPLC system (Waters Corp., Milford, MA) for linear gradient system 1 and a Hitachi L-6200A pump for linear gradient systems 2−5. The LC/UV experiments were performed using a Hitachi L-4200 UV detector at 263 nm. Gradient system 1 employed a YMC $C_{18}$ ODS-AQ column (150 mm × 2 mm i.d., 3 $\mu$m, 120 Å; YMC, Inc., Wilmington, NC) at a flow rate of 0.150 mL/min. Gradient systems 2−4 employed a YMC $C_{18}$ ODS-AQ column (250 mm × 4.6 mm i.d., 5 $\mu$m, 120 Å) at a flow rate of 1 mL/min. Gradient system 5 employed a YMC $C_{18}$ ODS-AQ column (250 mm × 10 mm i.d., 5 $\mu$m, 120 Å) at a flow rate of 2 mL/min. For system 1, solvent A was 5 mM ammonium acetate in water containing 0.1% (v/v) acetic acid, and solvent B was 5 mM ammonium acetate in methanol containing 0.1% (v/v) acetic acid. For systems 2−4, solvent A was 5 mM ammonium acetate in water containing 0.01% (v/v) trifluoroacetic acid, and solvent B was 5 mM ammonium acetate in methanol containing 0.01% (v/v) trifluoroacetic acid. For system 5, solvent A was 100% water, and solvent B was 100% methanol.

For system 1, the gradient conditions were as follows: 30% B at 0 min, 90% B at 18 min, 90% B at 19 min, 30% B at 20 min, followed by a 10 min equilibration time. For system 2, the gradient conditions were as follows: 30% B at 0 min, 45% B at 15 min, 75% B at 20 min, 30% B at 25 min, followed by a 5 min equilibration time. For system 3, the gradient conditions were as follows: 40% B at 0 min, 45% B at 15 min, 60% B at 25 min, and 40% B at 28 min. For system 4, the gradient conditions were as follows: 5% B at 0 min, 41% B at 5 min, 61% B at 20 min, 96% B at 23 min, 5% B at 24 min, followed by a 6 min equilibration time. For system 5, isocratic conditions were used with 20% A and 80% B.

**Synthesis of 4-Oxo-2-nonenal.** 4-Hydroxy-2-nonenal diethyl acetal was oxidized with activated $MnO_2$ as described by Esterbauer and Weger (*25*). The resulting 4-oxo-2-nonenal diethyl acetal was then hydrolyzed by citric acid/HCl as described previously (*11*).

**Reaction of 4-Oxo-2-nonenal with dCyd.** A solution of 4-oxo-2-nonenal (2000 $\mu$g, 13.0 $\mu$mol) in 15 $\mu$L of ethanol was added to dCyd (1500 $\mu$g, 6.6 $\mu$mol) in 250 $\mu$L of water. The reaction mixture was incubated at 37 °C for 24 h. An aliquot of the sample (10 $\mu$L) was diluted to 100 $\mu$L with water prior to analysis of 10 $\mu$L of the solution by LC/MS using gradient system 1.

In separate reactions, a solution of 4-oxo-2-nonenal (1600 $\mu$g, 10.4 $\mu$mol) in 15 $\mu$L of ethanol was added to dCyd (1300 $\mu$g, 5.7 $\mu$mol) in 250 $\mu$L of water. The reaction mixture was incubated at either 37 or 60 °C for 24 h, after which it was refrigerated at 4 °C. An aliquot of the sample (10 $\mu$L) was diluted to 100 $\mu$L with water prior to analysis of 10 $\mu$L of the solution by UV detection (263 nm) using gradient system 2. dCyd eluted at 4.9 min; adducts $A_1$ and $A_2$ eluted at 9.1 and 9.6 min, respectively; and adduct B eluted at 16.5 min.

**Preparation of Adducts $A_1$ and $A_2$ for LC/MS Analysis.** A solution of 4-oxo-2-nonenal (31.4 mg, 0.20 mmol) in 15 $\mu$L of ethanol was added to dCyd (5.4 mg, 0.02 mmol) in 300 $\mu$L of water. The reaction mixture was incubated at 37 °C for 24 h. At the end of the incubation, the reaction mixture was kept on ice, and the reaction products were isolated by preparative HPLC. Chromatography was performed using gradient system 3. The peaks at 16.0 and 17.4 min were collected as adducts $A_1$ and $A_2$, respectively. The adducts were stored at 4 °C and were used without further purification because of their stability.

**Preparation of Adduct B for UV and NMR Analysis.** A solution of 4-oxo-2-nonenal (50.5 mg, 0.33 mmol) in 500 $\mu$L of ethanol was added to dCyd (24.5 mg, 0.11 mmol) in 1000 $\mu$L of water. The reaction mixture was incubated at 60 °C for 20−24 h. After the reaction, the organic phase was extracted with diethyl ether, and adduct B was isolated from the aqueous phase using gradient system 5. The product that eluted at 9.1 min was collected as adduct B, concentrated under nitrogen at room temperature, recrystallized from acetonitrile, and dried under vacuum (yield, 27%).

**Transformation of Adducts $A_1$ and $A_2$ with Time.** Adducts $A_1$ and $A_2$ were shown to be >95% pure by LC/UV analysis. Sodium phosphate buffer (20 mM) was prepared at pH 5, 6, 7, and 8. In a 1.5 mL microcentrifuge tube, 100 $\mu$L of purified adduct $A_1$ solution was added to 300 $\mu$L of sodium phosphate solution adjusted to pH 5, resulting in a 15 mM sodium phosphate solution. The solution was then heated at 65 °C, and 40 $\mu$L was injected at 1, 2, 4, 6, and 24 h. The 0 h time point was taken from the purified adduct $A_1$ solution at 4 °C. Gradient system 4 was used for LC/UV analysis with monitoring at 278 nm ($\lambda_{max}$ of adduct B). The same steps were performed using the purified adduct $A_1$ solution at pH 6, 7, and 8. Also, the same procedure was used to analyze the transformation of the purified adduct $A_2$ solution.

## Results

**Reaction of 4-Oxo-2-nonenal with dCyd.** Using gradient system 1, LC/MS analysis of the products from the reaction between dCyd and 4-oxo-2-nonenal at 37 °C for 24 h revealed the presence of three major compounds with $MH^+$ ions at *m/z* 382 (adducts $A_1$ and $A_2$) and *m/z* 364 (adduct B) (Figure 1). In a separate reaction, LC/UV analysis (263 nm) of the products from the reaction at 37 °C for 24 h was performed. The resulting chromatogram confirmed the presence of three major products (adducts $A_1$, $A_2$, and B) together with residual dCyd (Figure 2). When the reaction was heated at 60 °C for 24 h, the magnitudes of the signals for adducts $A_1$ and $A_2$ were reduced considerably with a concomitant increase in the magnitude of the UV signal for adduct B (Figure 2).

**LC/MS Analysis of Adducts $A_1$ and $A_2$.** The mass spectra for adducts $A_1$ and $A_2$ were identical. Each spectrum exhibited an intense $MH^+$ ion at *m/z* 382. MS/MS analysis of *m/z* 382 at −25 eV resulted in several product ions, notably, a fragment ion at *m/z* 266 that resulted from the loss of 2′-deoxyribose (−116). This suggested that the modification had occurred on the pyrimidine moiety. Product ions were also observed as follows: *m/z* 248 ($BH_2^+ - H_2O$), *m/z* 150 ($BH_2^+ - H_2O - C_5H_{11}CO$), and *m/z* 112 (Cyt) (Figure 3). These mass

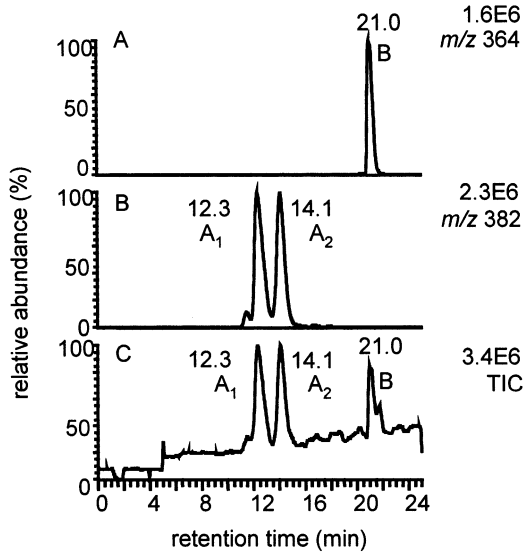


**Figure 1.** Analysis of the reaction mixture between 4-oxo-2-nonenal and dCyd after 24 h of incubation at 37 °C by LC/MS in ESI mode using gradient system 1. (A) Selected ion chromatogram for the $MH^+$ of adduct B (*m/z* 364). (B) Selected ion chromatogram for the $MH^+$ of adducts $A_1$ and $A_2$ (*m/z* 382). (C) Total ion current chromatogram for the reaction mixture.

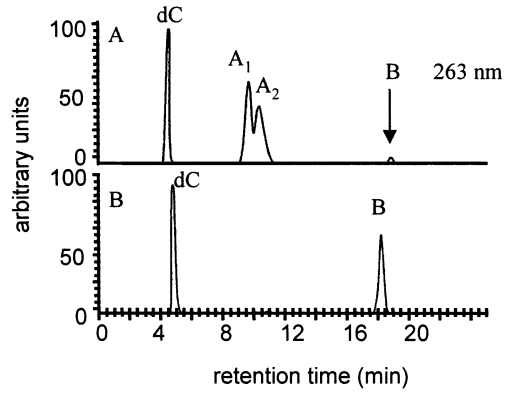


**Figure 2.** Analysis of the reaction mixture between 4-oxo-2-nonenal and dCyd after 24 h of incubation monitored by UV at 263 nm using gradient system 2. (A) HPLC chromatogram of the reaction mixture incubated at 37 °C. (B) HPLC chromatogram of the reaction mixture incubated at 60 °C.

spectral characteristics were consistent with diastereomeric substituted ethano−dCyd adducts.

**LC/MS Analysis of Adduct B.** The mass spectrum of adduct B exhibited an intense $MH^+$ ion at *m/z* 364. MS/MS analysis of *m/z* 364 at −50 eV resulted in a $BH_2^+$ ion at *m/z* 248, along with several product ions at *m/z* 150 ($BH_2^+ - C_5H_{11}CO$), *m/z* 149, and *m/z* 121 (Figure 4). These data were consistent with the proposal that adduct B was a dehydration product of adducts $A_1$ and $A_2$.

**UV Analysis of Adduct B.** Adduct B exhibited a $\lambda_{max}$ of 278 nm ($\epsilon = 1.25 \times 10^4\ M^{-1}\ cm^{-1}$) at pH 7.0. The $\lambda_{max}$ was shifted to 299 nm ($\epsilon = 1.12 \times 10^4\ M^{-1}\ cm^{-1}$) at pH 1, but the $\lambda_{max}$ was not shifted ($\epsilon = 1.20 \times 10^4\ M^{-1}\ cm^{-1}$) at pH 13 (Figure 5).

**NMR Analysis of Adduct B.** Assignments were made on the basis of chemical shifts and proton−proton couplings (Table 1) together with COSY, HSQC, and HMBC correlations (Table 2). Besides the aromatic AB system of the dCyd moiety, there was an additional aromatic proton singlet at 7.09 ppm (H-8) (Figure 6). This proton showed COSY correlations with the methylene protons

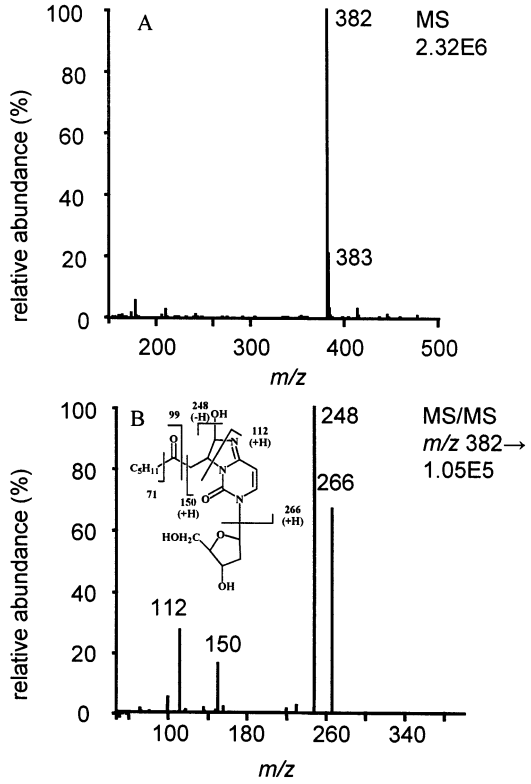


**Figure 3.** LC/MS/MS analysis of adduct $A_1$ using ESI mode. The spectrum for $A_1$ was identical for $A_2$. (A) Full scan mass spectrum; (B) MS/MS spectrum.

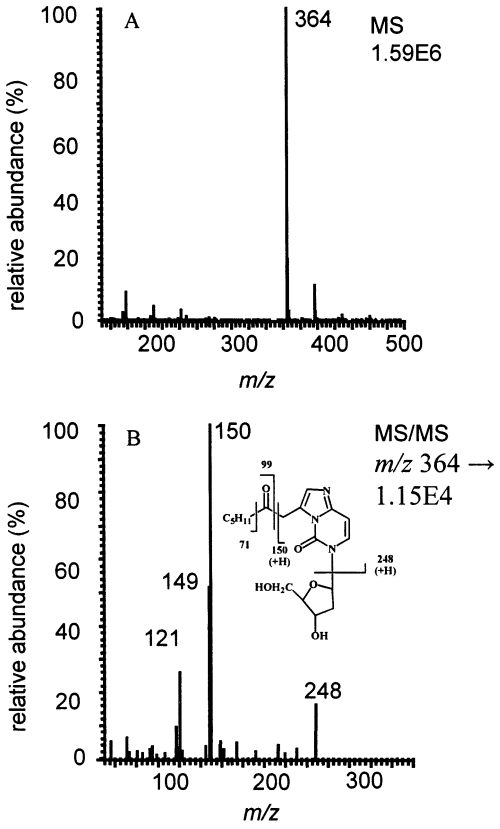


**Figure 4.** LC/MS/MS analysis of adduct B using ESI mode. (A) Full scan mass spectrum; (B) MS/MS spectrum.

at C-1″ (4.13 and 4.09 ppm) (Figure 7). These data were consistent with the presence of an olefinic bond between C-8 and C-9 (Figure 9). The triplet at 2.49 ppm was

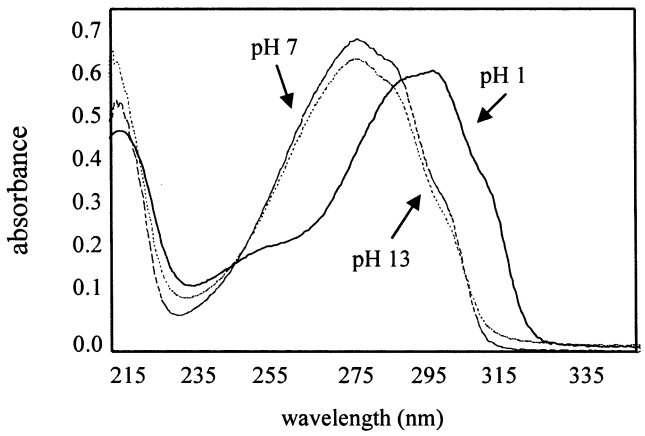


**Figure 5.** UV spectra of adduct B at pH 1, 7, and 13.

**Table 1. $^1$H NMR Assignments for Adduct B[a]**

| assigned H | $\delta$ (ppm) | multiplet | H-coupled ($J$, Hz) | type |
|---|---|---|---|---|
| H-6 | 7.60 | doublet | H-5 (7.9) | N−C*H*= |
| H-8 | 7.09 | singlet | | N−C*H*= |
| H-5 | 6.61 | doublet | H-6 (7.9) | C−C*H*= |
| H-1′ | 6.28 | triplet | H-2′a (6.8), H-2′b (6.8) | −NC*H*O |
| 3′-OH | 5.25 | doublet | H-3′ (4.1) | −CHO*H* |
| 5′-OH | 5.03 | triplet | H-5′a (5.1), H-5′b (5.1) | −CH$_2$O*H* |
| H-3′ | 4.25 | multiplet | | −OC*H*− |
| H-1″b | 4.13 | doublet | H-1″a (17.8) | −C*H*$_2$−C |
| H-1″a | 4.09 | doublet | H-1″b (17.8) | −C*H*$_2$−C |
| H-4′ | 3.80 | multiplet | | −C*H*O |
| H-5′a,b | 3.57 | multiplet | | −C*H*$_2$O |
| H-3″a,b | 2.49 | triplet | H-4″a (7.4), H-4″b (7.4) | −C*H*$_2$−C |
| H-2′a,b | 2.12 | multiplet | | −C*H*$_2$−C |
| H-4″a,b | 1.47 | multiplet | | −C*H*$_2$−C |
| H-6″a,b | 1.24 | multiplet | | −C*H*$_2$−C |
| H-5″a,b | 1.20 | multiplet | | −C*H*$_2$−C |
| H-7″ | 0.84 | triplet | H-6″a (7.0), H-6″b (7.0) | −C*H*$_3$ |

[a] Spectra were obtained in DMSO-$^2$H$_6$.

assigned to the methylene protons at C-3″ because of its chemical shift and its multiplicity (Figure 6). The COSY spectrum showed the correlations between the C-3″ protons with the C-4″ protons (1.47 ppm), the C-4″ protons and the C-5″ protons (1.20 ppm), the C-5″ protons with the C-6″ protons (1.24 ppm), and, finally, the C-6″ protons with the methyl group at C-7″ (0.84 ppm) (Figure 7). The COSY spectrum also showed the correlations of the protons of the furanosyl moiety. This spectrum showed correlations between the H-1′ proton (6.28 ppm) and the protons at C-2′ (2.12 ppm), the C-2′ protons with the C-3′ proton (4.25 ppm), the C-3′ protons with the hydroxyl at C-3′ (5.25 ppm) and with the C-4′ proton (3.80 ppm), the C-4′ proton with the C-5′ protons (3.57 ppm), and the C-5′ protons with the hydroxyl at C-5′ (5.03 ppm) (Figure 7).

**Table 2. $^{13}$C NMR Assignments for Adduct B[a]**

| assigned carbon | $\delta$ (ppm) | type | assigned carbon | $\delta$ (ppm) | type |
|---|---|---|---|---|---|
| C-7″ | 13.6 | −*C*H$_3$ | C-1′ | 84.6 | N−*C*HO− |
| C-6″ | 21.5 | −*C*H$_2$− | C-4′ | 87.5 | −*C*HO |
| C-4″ | 22.4 | −*C*H$_2$− | C-5 | 98.7 | −*C*H= |
| C-5″ | 30.3 | −*C*H$_2$− | C-9 | 122.9 | −N−*C*= |
| C-1″ | 38.8 | −*C*H$_2$− | C-6 | 127.6 | −N−*C*H= |
| C-2′ | 39.7 | −*C*H$_2$− | C-8 | 132.5 | −N−*C*H= |
| C-3″ | 40.9 | −*C*H$_2$− | C-4 | 145.0 | −N−*C*=N |
| C-5′ | 61.1 | −*C*H$_2$−O | C-2 | 146.7 | N−*C*=O |
| C-3′ | 70.2 | −*C*H−O | C-2″ | 206.2 | −*C*=O |

[a] Spectra were obtained in DMSO-$^2$H$_6$.

Cycloaddition of 4-oxo-2-nonenal to dCyd can result in addition of the heptanone chain at the C-8 or C-9 position. To elucidate the mechanism of adduction, HMBC experiments were performed. HMBC was carried out at three different long-range C−H coupling constants ($^3J^1$H−$^{13}$C = 5, 7, and 10 Hz). If the heptanone chain was attached to the C-8 position, the key three bond C−H correlation would be H-9 with C-2 and C-4. If the heptanone chain was attached to the C-9 position, the three bond C−H correlation would be H-8 with only C-4. Assignments of C-2 (146.7 ppm) and C-4 (145.0 ppm) through the H-6/C-4, H-5/C-4, H-8/C-4, H-1′/C-2, and H-6/C-2 HMBC correlations were essential for this analysis. Indeed, HMBCs showed only the correlation between H-8 and C-4 (Figure 8), indicating that the heptanone chain is attached to the C-9 position, not C-8. Thus, the structure consistent with the NMR data is 1″-[1-(2′-deoxy-$\beta$-D-*erythro*-pentofuranosyl)-1H-imidazo[2,1-c]pyrimidin-2-oxo-4-yl]heptane-2″-one (Figure 9).

**Transformation of Adducts $A_1$ and $A_2$.** A time course experiment performed at 65 °C and at pH 5−8 revealed the following: By the 6 h time point, adducts $A_1$ and $A_2$ had been primarily converted to either adduct B or dCyd. Interestingly, the transformation of both adducts was found to be pH-dependent. At pH 5 and pH 6, adduct $A_1$ dehydrated to primarily adduct B (Figure 10). At pH 7, adduct $A_1$ converted to both dCyd and adduct B (Figure 10). Finally, at pH 8, adduct $A_1$ hydrolyzed to primarily dCyd (Figure 10). Adduct $A_2$ behaved in an identical manner (data not shown).

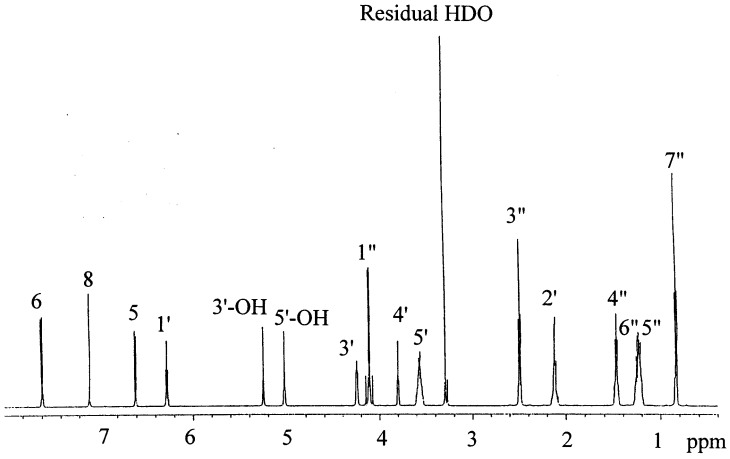


**Figure 6.** $^1$H NMR spectrum of adduct B (DMSO-$^2$H$_6$, 600 MHz).

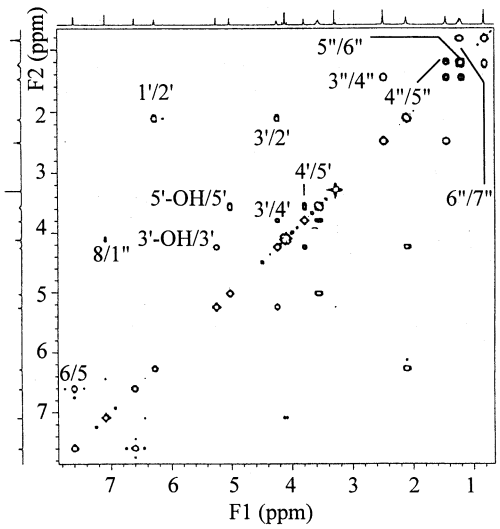


**Figure 7.** COSY spectrum (DMSO-$^2H_6$, 600 MHz).

## Discussion

We recently identified 4-oxo-2-nonenal as a novel product of lipid peroxidation (*6*). In previous studies, we characterized substituted etheno−dGuo and etheno−dAdo adducts (*11*−*13*) that arose through sequential nucleophilic additions to 4-oxo-2-nonenal. In this study, analysis of the reaction between 4-oxo-2-nonenal and dCyd revealed the presence of three major products (adducts $A_1$, $A_2$, and B). Adducts $A_1$ and $A_2$ were consistent with substituted ethano−dCyd adducts (Figure 3), and adduct B was characterized as a 7-heptanone-etheno−dCyd adduct by LC/MS and NMR spectroscopy (Figure 9). In acidic conditions, adduct $A_1$ was transformed primarily to adduct B (Figure 10). In basic conditions, however, adduct $A_1$ was hydrolyzed primarily to dCyd (Figure 10). Adduct $A_2$ behaved in an identical manner to adduct $A_1$ (data not shown). Hydrolysis of adducts $A_1$ and $A_2$ to dCyd most likely occurs by a retro-aldol reaction as depicted in Figure 11. We propose that 4-oxo-2-nonenal reacted with dCyd as follows: initially, nucleophilic addition of $N^4$ from dCyd occurred at aldehyde C-1. This was followed by reaction of N-3 at C-2 of the resulting α,*β*-unsaturated ketone to generate adducts $A_1$ and $A_2$, diastereomers of one another. Subsequent dehydration of adducts $A_1$ and $A_2$ resulted in the formation of adduct B (Figure 12). Our data, however, could not distinguish between initial Michael addition of N-3 at C-2 of the α,*β*-unsaturated aldehyde followed by nucleophilic addition of $N^4$ at aldehyde C-1.

Etheno adducts can be formed from reaction of the nucleic acid base with a number of structurally diverse chemicals, including vinyl chloride, urethane (ethyl carbamate), halogenated aldehydes, and other compounds (*26*). In 1974, vinyl chloride was shown to be a human carcinogen that induced angiosarcoma of the liver, a very rare type of tumor (*27*). Subsequently, vinyl chloride was found to be metabolized to chloroethylene oxide and chloroacetaldehyde, both of which proved to be mutagenic (*28*). The unsubstituted etheno adducts were subsequently shown to possess in vitro miscoding properties (*29*−*31*).

Following these early in vitro mutagenesis studies, researchers began to develop an analytical methodology to detect unsubstituted etheno adducts in vivo. The adducts were shown to occur in rodents and humans exposed to environmental carcinogens, such as vinyl

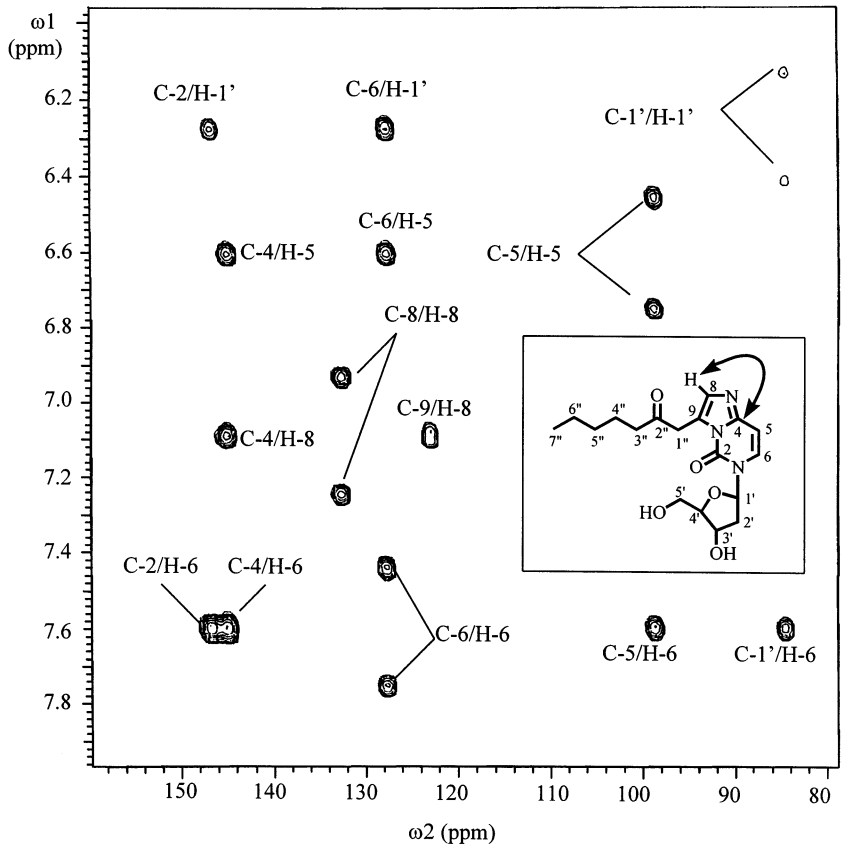


**Figure 8.** HMBC spectrum, optimized $^3J^1H$-$^{13}C$ = 7 Hz (DMSO-$^2H_6$, 600 MHz).

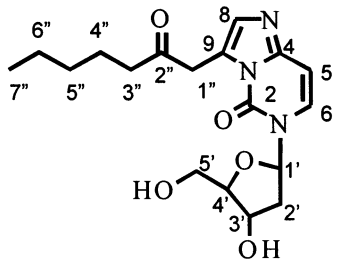

**I**

**Figure 9.** Structure of adduct B based on NMR data.

chloride (*32*, *33*). More recently, however, using immunoaffinity and the $^{32}$P-postlabeling method, it was found that these etheno adducts were also formed endogenously (*15*, *34*); the unsubstituted etheno−dCyd adduct has been detected in human liver samples and human urine (*35*−*37*). In relation to cancer, increased levels of etheno adducts have been found in colon polyps from patients with familial adenomatous polyposis (*16*). Also, increased levels of etheno−dAdo and etheno−dCyd adducts have been found in the mouse skin two stage model of carcinogenesis. In fact, use of the tumor promoter TPA in this model led to an increase of 12- and 9-fold in etheno−dAdo and etheno−dCyd, respectively (*17*).

The endogenous source of etheno adducts is thought to be from breakdown products from lipid peroxidation. In 1988, Sodum and Chung showed that 1,$N^2$-etheno-Guo could be formed in vitro by *trans*-4-hydroxy-2-nonenal in the presence of hydroperoxide (*38*). They later showed that 2,3-epoxy-4-hydroxynonanal, resulting from epoxidation of *trans*-4-hydroxy-2-nonenal, could form the etheno adduct (*39*). Similarly, other in vitro studies have shown that peroxide treatment of 4-hydroxy-2-nonenal and *trans*,*trans*-2,4-decadienal results in the formation of etheno adducts (*40*−*42*). It is unclear, however, if such peroxidation reactions occur in vivo due to competition by detoxification enzymes, such as glutathione-S-transferases and aldo-keto reductases (*43*). Alternatively, unsubstituted etheno adducts can be formed from *trans*-4,5-epoxy-2(*E*)-decenal, without the need for an additional oxidation step. In vitro reactions with *trans*-4,5-epoxy-2(*E*)-decenal and dAdo or dGuo resulted in the formation of 1,$N^6$-etheno-dAdo and 1,$N^2$-etheno-dGuo, respectively (*44*).

In regards to the unsubstituted etheno−dCyd adduct, studies investigating its mutagenic potential were conducted using in vitro primer extension assays. Studies using the Klenow fragment of the *E. coli* DNA polymerase I showed that dAMP, followed by dTMP, was preferentially incorporated opposite the etheno−dCyd lesion; thus, the unsubstituted etheno−dCyd adduct led predominantly to C → T transitions and C → A transversions (*18*, *19*). More recently, etheno−dCyd has been studied using mammalian DNA polymerases, such as Pol α, *β*, and *δ*. Pol α primarily catalyzed incorporation of dTMP and dAMP opposite etheno−dCyd; Pol *β* primarily catalyzed incorporation of dCMP and dAMP; and Pol *δ* primarily catalyzed incorporation of dTMP (*20*).

Adduct site specific mutagenesis studies on etheno−dCyd were initially conducted in *E. coli*. A single etheno−dCyd adduct was introduced into M13 viral DNA, and then, the DNA was transfected into *E. coli*. Frequency and specificity of mutations induced by etheno−dCyd were analyzed by direct sequencing of progeny phage plaques. In one study, only C → T transitions and C → A transversions were observed (*22*). In a similar study, mutations were mainly C → T transitions, with targeted C → A transversions and −1 base deletions also detected. The mutation frequency due to etheno−dCyd was 1.5−2% (*23*). In a different approach using a single-stranded vector containing a single etheno−dCyd adduct, Moriya et al. determined that etheno−dCyd resulted primarily in C → A transversions and C → T transitions. This study confirmed the low mutation rate in nonirradiated *E. coli* (∼2%); surprisingly, however, etheno−dCyd resulted in a targeted mutation frequency of 81% in simian kidney (COS) cells (*24*). The biological relevance of the substituted etheno−dCyd adduct identified in the present study has yet to be established. Therefore, ongoing studies in

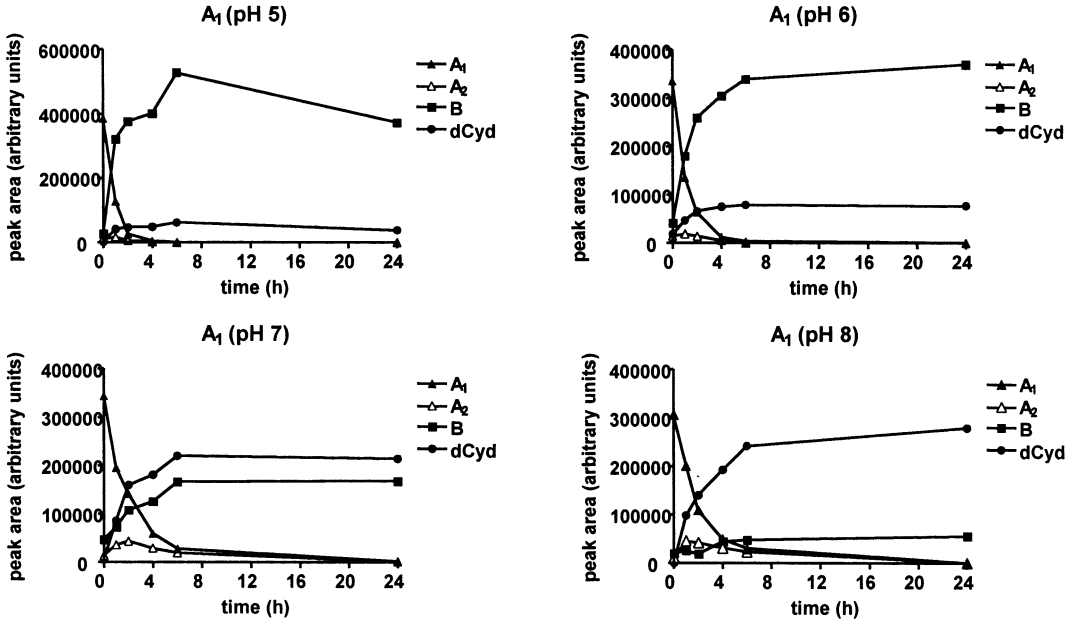


**Figure 10.** Time courses for the transformation of adduct $A_1$ with different pH values.

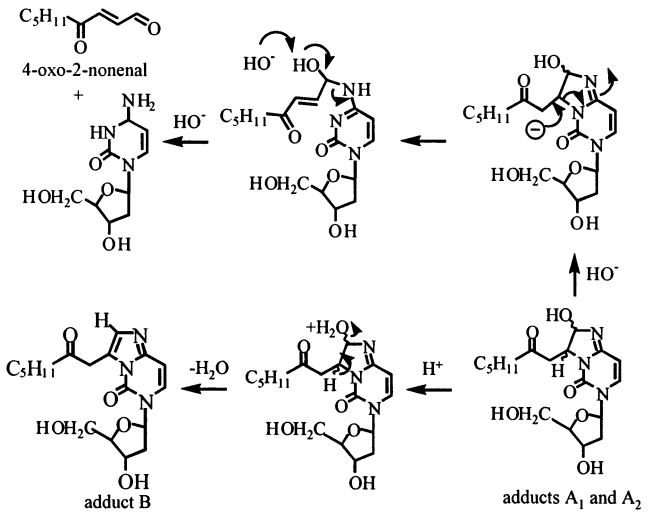


**Figure 11.** Proposed transformation mechanism of adducts $A_1$ and $A_2$ in acidic and basic conditions.

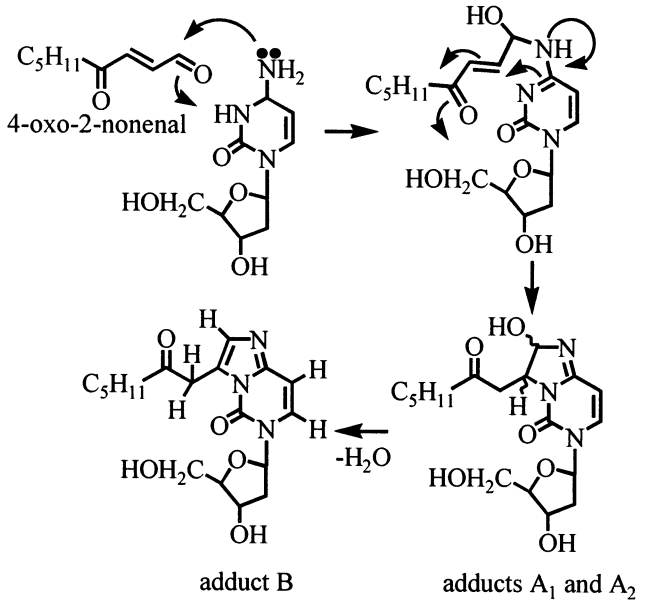


**Figure 12.** Proposed mechanism of formation of adducts $A_1$, $A_2$, and B.

our laboratory are examining its blocking and miscoding properties.

**Acknowledgment.** We thank Dr. Hye-Young Kim for many helpful discussions. We gratefully acknowledge financial support from the National Institutes of Health in the form of an RO1 Grant to I.A.B. (CA91016).

## References

(1) Ames, B. N., Gold, L. S., and Willett, W. C. (1995) The causes and prevention of cancer. *Proc. Natl. Acad. Sci. U.S.A.* **92**, 5258−5265.

(2) Marnett, L. J. (2000) Oxyradicals and DNA damage. *Carcinogenesis* **21**, 361−370.

(3) Porter, N. A., Caldwell, S. E., and Mills, K. A. (1995) Mechanisms of free radical oxidation of unsaturated lipids. *Lipids* **30**, 277−290.

(4) Hsi, L. C., Wilson, L., Nixon, J., and Eling, T. E. (2001) 15-Lipoxygenase-1 metabolites down-regulate peroxisome proliferator-activated receptor g via the MAPK signaling pathway. *J. Biol. Chem.* **276**, 34545−34552.

(5) Marnett, L. J., and DuBois, R. N. (2002) COX-2: a target for colon cancer prevention. *Annu. Rev. Pharmacol. Toxicol.* **42**, 55−80.

(6) Lee, S. H., and Blair, I. A. (2000) Characterization of 4-oxo-2-nonenal as a novel product of lipid peroxidation. *Chem. Res. Toxicol.* **13**, 698−702.

(7) Lee, S. H., Oe, T., and Blair, I. A. (2001) Vitamin C-induced decomposition of lipid hydroperoxides to endogenous genotoxins. *Science* **292**, 2083−2086.

(8) Blair, I. A. (2001) Lipid hydroperoxide-mediated DNA damage. *Exp. Gerontol.* **36**, 1473−1481.

(9) Burcham, P. C. (1998) Genotoxic lipid peroxidation products: their DNA damaging properties and role in formation of endogenous DNA adducts. *Mutagenesis* **13**, 287−305.

(10) Winter, C. K., Segall, H. J., and Haddon, W. F. (1986) Formation of cyclic adducts of deoxyguanosine with the aldehydes *trans*-4-hydroxy-2-hexenal and *trans*-4-hydroxy-2-nonenal in vitro. *Cancer Res.* **46**, 5682−5686.

(11) Rindgen, D., Nakajima, M., Wehrli, S., Xu, K., and Blair, I. A. (1999) Covalent modifications to 2′-deoxyguanosine by 4-oxo-2-nonenal a novel product of lipid peroxidation. *Chem. Res. Toxicol.* **12**, 1195−1204.

(12) Rindgen, D., Lee, S. H., Nakajima, M., and Blair, I. A. (2000) Formation of a substituted 1,$N^6$-etheno-2′-deoxyadenosine adduct by lipid hydroperoxide-mediated generation of 4-oxo-2-nonenal. *Chem. Res. Toxicol.* **13**, 846−852.

(13) Lee, S. H., Rindgen, D., Bible, R. A., Hajdu, E., and Blair, I. A. (2000) Characterization of 2′-deoxyadenosine adducts derived from 4-oxo-2-nonenal, a novel product of lipid peroxidation. *Chem. Res. Toxicol.* **13**, 565−574.

(14) Green, T., and Hathway, D. E. (1978) Interactions of vinyl chloride with rat-liver DNA in vivo. *Chem.-Biol. Interact.* **22**, 211−224.

(15) Nair, J., Barbin, A., Guichard, Y., and Bartsch, H. (1995) 1,$N^6$-ethenodeoxyadenosine and 3,$N^4$-ethenodeoxycytidine in liver DNA from humans and untreated rodents detected by immunoaffinity/$^{32}$P-postlabeling. *Carcinogenesis* **16**, 613−617.

(16) Schmid, K., Nair, J., Winde, G., Velic, I., and Bartsch, H. (2000) Increased levels of promutagenic etheno-DNA adducts in colonic polyps of FAP patients. *Int. J. Cancer* **87**, 1−4.

(17) Nair, J., Fürstenberger, G., Bartsch, H., Marks, F., and Bartsch (2000) Promutagenic etheno-DNA adducts in multistage mouse skin carcinogenesis: Correlation with lipoxygenase-catalyzed arachidonic acid metabolism. *Chem. Res. Toxicol.* **13**, 703−709.

(18) Simha, D., Palejwala, V. A., and Humayun, M. Z. (1991) Mechanisms of mutagenesis by exocyclic DNA adducts. Construction and in vitro template characteristics of an oligonucleotide bearing a single site-specific ethenocytosine. *Biochemistry* **30**, 8727−8735.

(19) Zhang, W., Johnson, F., Grollman, A., and Shibutani, S. (1995) Miscoding by the exocyclic and related DNA adducts 3,$N^4$-etheno-2′-deoxycytidine, 3,$N^4$-ethano-2′-deoxycytidine, and 3-(2-hydroxyethyl)-2′-deoxyuridine. *Chem. Res. Toxicol.* **8**, 157−163.

(20) Shibutani, S., Suzuki, N., Matsumoto, Y., and Grollman, A. P. (1996) Miscoding properties of 3,$N^4$-etheno-2′-deoxycytidine in reactions catalyzed by mammalian DNA polymerases. *Biochemistry* **35**, 14992−14998.

(21) Singer, B., Medina, M., Zhang, Y., Wang, Z., Guliaev, A. B., and Hang, B. (2002) 8-(Hydroxymethyl)-3,$N^4$-etheno-C, a potential carcinogenic glycidaldehyde product, miscodes in vitro using mammalian DNA polymerases. *Biochemistry* **41**, 1778−1785.

(22) Palejwala, V. A., Simha, D., and Humayun, M. Z. (1991) Mechanisms of mutagenesis by exocyclic DNA adducts. Transfection of M13 viral DNA bearing a site specific adduct shows that ethenocytosine is a highly efficient RecA-independent mutagenic noninstructional lesion. *Biochemistry* **30**, 8736−8743.

(23) Basu, A. K., Wood, M. L., Niedernhofer, L. J., Ramos, L. A., and Essigmann, J. M. (1993) Mutagenic and genotoxic effects of three vinyl chloride-induced DNA lesions: 1,$N^6$-ethenoadenine, 3,$N^4$-ethenocytosine, and 4-amino-5- (imidazol-2-yl)imidazole. *Biochemistry* **32**, 12793−12801.

(24) Moriya, M., Zhang, W., Johnson, F., and Grollman, A. P. (1994) Mutagenic potency of exocyclic DNA adducts: marked differences between *Escherichia coli* and simian kidney cells. *Proc. Natl. Acad. Sci. U.S.A.* **91**, 11899−11903.

(25) Esterbauer, H., and Weger, W. (1967) Über die wirkungen von aldehyden auf gesunde und maligne zellen, 3. mitt.: synthese von homologen 4-hydroxy-2-alkenalen, II. *Monatsh. Chem.* **98**, 1994−2000.

(26) Barbin, A. (2000) Etheno-adduct-forming chemicals: from mutagenicity testing to tumor mutation spectra. *Mutat. Res.* **462**, 55−69.

(27) Creech, J. L., Jr., and Johnson, M. N. (1974) Angiosarcoma of liver in the manufacture of poly(vinyl chloride). *J. Occup. Med.* **16**, 150−151.

(28) Malaveille, C., Bartsch, H., Barbin, A., Camus, A. M., Montesano, R., Croisy, A., and Jacquignon, P. (1975) Mutagenicity of vinyl chloride, chloroethyleneoxide, chloroacetaldehyde and chloroethanol. *Biochem. Biophys. Res. Commun.* **63**, 363−370.

(29) Barbin, A., Bartsch, H., Leconte, P., and Radman, M. (1981) Studies on the miscoding properties of 1,$N^6$-ethenoadenine and 3,$N^4$- ethenocytosine, DNA reaction products of vinyl chloride metabolites, during in vitro DNA synthesis. *Nucleic Acids Res.* **9**, 375−387.

(30) Hall, J. A., Saffhill, R., Green, T., and Hathway, D. E. (1981) The induction of errors during in vitro DNA synthesis following chloroacetaldehyde-treatment of poly(dA-dT) and poly(dC-dG) templates. *Carcinogenesis* **2**, 141−146.

(31) Spengler, S., and Singer, B. (1981) Transcriptional errors and ambiguity resulting from the presence of 1,$N^6$-ethenoadenosine or 3,$N^4$-ethenocytidine in polyribonucleotides. *Nucleic Acids Res.* **9**, 365−373.

(32) Eberle, G., Barbin, A., Laib, R. J., Ciroussel, F., Thomale, J., Bartsch, H., and Rajewsky, M. F. (1989) 1,$N^6$-etheno-2′-deoxyadenosine and 3,$N^4$-etheno-2′-deoxycytidine detected by monoclonal antibodies in lung and liver DNA of rats exposed to vinyl chloride. *Carcinogenesis* **10**, 209−212.

(33) Fedtke, N., Boucheron, J. A., Turner, M. J., Jr., and Swenberg, J. A. (1990) Vinyl chloride-induced DNA adducts. I: Quantitative determination of $N^{2,3}$-ethenoguanine based on electrophore labeling. *Carcinogenesis* **11**, 1279−1285.

(34) Bartsch, H., Barbin, A., Marion, M. J., Nair, J., and Guichard, Y. (1994) Formation, detection, and role in carcinogenesis of etheno-bases in DNA. *Drug Metab. Rev.* **26**, 349−371.

(35) Bartsch, H., and Nair, J. (2000) New DNA-based biomarkers for oxidative stress and cancer chemoprevention studies. *Eur. J. Cancer* **36**, 1229−1234.

(36) Chen, H. J., Lin, T. C., Hong, C. L., and Chiang, L. C. (2001) Analysis of 3,$N^4$-ethenocytosine in DNA and in human urine by isotope dilution gas chromatography/negative ion chemical ionization/mass spectrometry. *Chem. Res. Toxicol.* **14**, 1612−1619.

(37) Churchwell, M. I., Beland, F. A., and Doerge, D. R. (2002) Quantification of multiple DNA adducts formed through oxidative stress using liquid chromatography and electrospray tandem mass spectrometry. *Chem. Res. Toxicol.* **15**, 1295−1301.

(38) Sodum, R. S., and Chung, F. L. (1988) 1,$N^2$-ethenodeoxyguanosine as a potential marker for DNA adduct formation by *trans*-4-hydroxy-2-nonenal. *Cancer Res.* **48**, 320−323.

(39) Sodum, R. S., and Chung, F.-L. (1991) Stereoselective formation of in vitro nucleic acid adducts by 2,3-epoxy-4-hydroxynonanal. *Cancer Res.* **51**, 137−143.

(40) Chen, H.-J. C., and Chung, F.-L. (1994) Formation of etheno adducts in reactions of enals via autoxidation. *Chem. Res. Toxicol.* **7**, 857−860.

(41) Carvalho, V. M., Asahara, F., Di Mascio, P., de Arruda Campos, I. P., Cadet, J., and Medeiros, M. H. G. (2000) Novel 1,$N^6$-etheno-2′-deoxyadenosine adducts from lipid peroxidation products. *Chem. Res. Toxicol.* **13**, 397−405.

(42) Loureiro, A. P. M., Di Mascio, P., Gomes, O. F., and Medeiros, M. H. G. (2000) *trans*,*trans*-2,4-decadienal-induced 1,$N^2$-etheno-2′-deoxyguanosine adduct formation. *Chem. Res. Toxicol.* **13**, 601−609.

(43) Burczynski, M. E., Sridhar, G. R., Palackal, N. T., and Penning, T. M. (2001) The reactive oxygen species- and Michael acceptor-inducible human aldo-keto reductase AKR1C1 reduces the α,β-unsaturated aldehyde 4-hydroxy-2-nonenal to 1,4-dihydroxy-2-nonene. *J. Biol. Chem.* **276**, 2890−2897.

(44) Lee, S. H., Oe, T., and Blair, I. A. (2002) 4,5-Epoxy-2(*E*)-decenal-induced formation of 1,$N^6$-etheno-2′-deoxyadenosine and 1,$N^2$-etheno-2′-deoxyguanosine adducts. *Chem. Res. Toxicol.* **15**, 300−304.

TX030009P